

# 194777: quartzofeldspathic gneiss, Mount Malcolm

(*Snowys Dam Formation, Arid Basin, Albany–Fraser Orogen*)

## Location and sampling

NORSEMAN (SI 51-2), FRASER RANGE (3433)  
MGA Zone 51, 483364E 6433838N

Sampled on 16 October 2009

This sample was collected from a ridge south of an east-trending track on Southern Hills Station, about 5.4 km northwest of Bobbys Tank, 3.9 km south of Southern Hills Homestead, and 1.2 km southwest of Mount Malcolm.

## Tectonic unit/relations

The unit sampled is a garnet-bearing quartzofeldspathic gneiss assigned to the Snowys Dam Formation of the Arid Basin. The Snowys Dam Formation is intruded by sheets of granitic and gabbroic rocks of the Fraser Zone and, collectively, these rocks define the Fraser Range Metamorphics (Spaggiari et al., 2011). The Fraser Range Metamorphics underwent amphibolite- to granulite-facies metamorphism during Stage I of the Albany–Fraser Orogeny (Clark et al., 1999; DeWaele and Pisarevsky, 2008; Spaggiari et al., 2011). Magmatic crystallization of a gabbro within the Fraser Zone was previously dated at  $1291 \pm 8$  Ma, by SHRIMP U–Pb analyses of zircons (De Waele and Pisarevsky, 2008). Early metamorphism in the Fraser Zone, at  $1304 \pm 7$  Ma, was recorded by zircon rims developed within a quartz metasandstone, which also yielded a maximum depositional age of  $1466 \pm 17$  Ma (GSWA 177910, Wingate and Bodorkos, 2007). This quartzofeldspathic gneiss is interlayered with mafic iron-rich metasedimentary rocks. The quartzofeldspathic layers have high titanium and calcium content. A date of  $1285 \pm 7$  Ma was determined for leucosome crystallization (GSWA 194715, Kirkland et al., 2011b) within metasedimentary rocks of the Snowys Dam Formation that yielded a maximum depositional age ( $1\sigma$ ) of  $1334 \pm 20$  Ma (GSWA 194714, Kirkland et al., 2011a)..

## Petrographic description

The sample is a quartzofeldspathic gneiss, composed of about 40% quartz, 30% plagioclase (oligoclase, An<sub>28</sub>) and perthite, 15% garnet, 10% hypersthene, 4% opaque oxide minerals, and accessory zircon, biotite, epidote, sillimanite, and sericite. Quartz is mostly less than 0.5 mm in diameter, although sparse elongate grains are up to 1 mm long. Garnet forms medium-grained anhedral poikilitic grains containing inclusions of quartz.

Hypersthene shows faint pink and green pleochroism and is fractured and altered by biotite and hematite-stained chlorite, and contains inclusions of sheafs of acicular sillimanite. Iron oxide minerals are commonly associated with altered pyroxene. Hypersthene–garnet assemblages represent high-temperature and high-pressure metamorphism.

## Zircon morphology

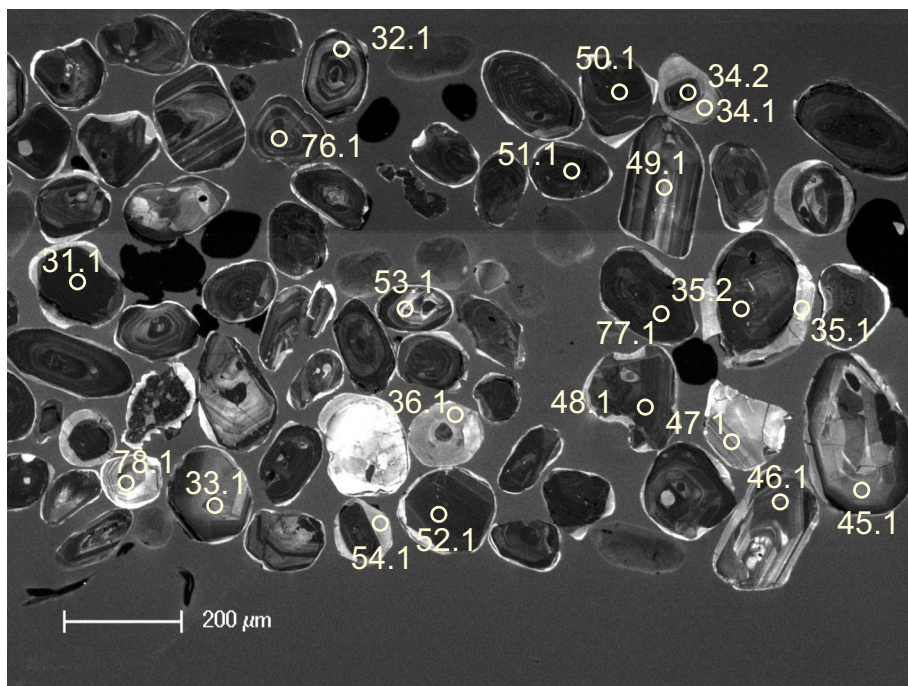
Zircons isolated from this sample are subhedral to euhedral, colourless to pale brown, up to 300 µm, and slightly elongate, with aspect ratios up to 5:1. In cathodoluminescence (CL) images, idiomorphic zoning is ubiquitous and some crystals are overgrown by narrow, low-uranium rims. A CL image of representative zircons is shown in Figure 1.

## Analytical details

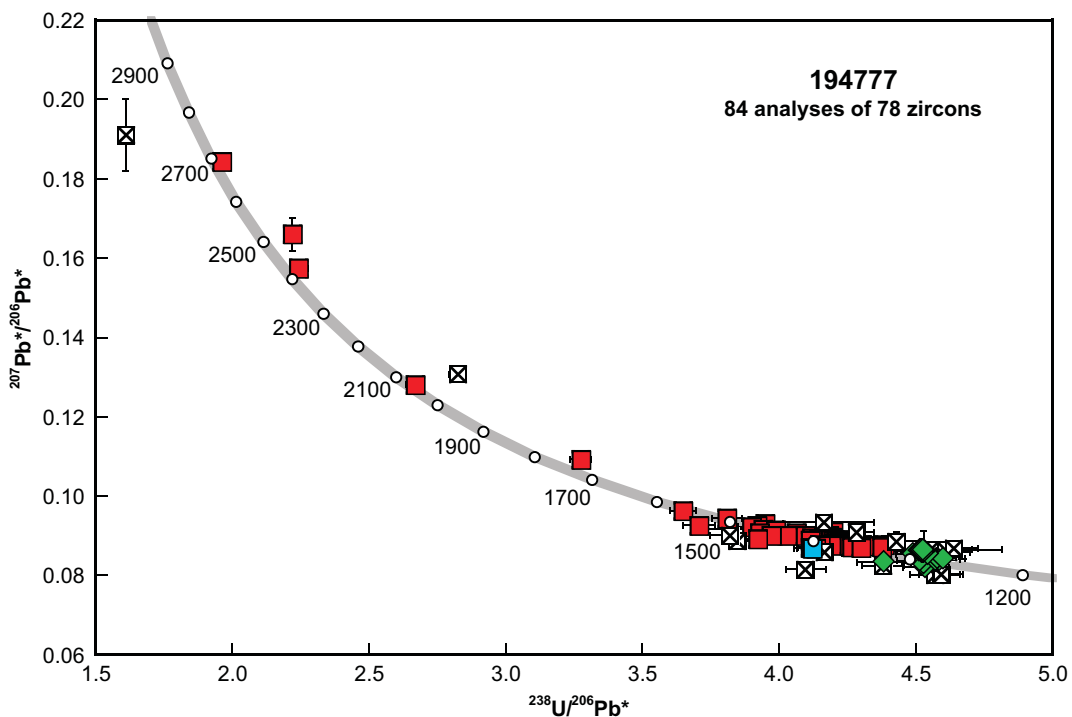
This sample was analysed on 17–18 June 2011 and on 23–24 June 2011, using SHRIMP-A, and on 30 June – 1 July 2011, using SHRIMP-B. Analyses 1.1 to 6.1 (spot numbers 1–6) were obtained during the first session, together with seven analyses of the BR266 standard, of which six analyses indicated an external spot-to-spot (reproducibility) uncertainty of 0.58% ( $1\sigma$ ) and a  $^{238}\text{U}/^{206}\text{Pb}^*$  calibration uncertainty of 0.26% ( $1\sigma$ ). Analyses 6.2 to 44.1 (spot numbers 7–48) were obtained during the second session, together with 16 analyses of the BR266 standard, of which 13 analyses indicated an external spot-to-spot (reproducibility) uncertainty of 1.07% ( $1\sigma$ ) and a  $^{238}\text{U}/^{206}\text{Pb}^*$  calibration uncertainty of 0.31% ( $1\sigma$ ). Analyses 45.1 to 78.1 (spot numbers 49–84) were obtained during the second session, together with 12 analyses of the BR266 standard, of which 10 analyses indicated an external spot-to-spot (reproducibility) uncertainty of 0.92% ( $1\sigma$ ) and a  $^{238}\text{U}/^{206}\text{Pb}^*$  calibration uncertainty of 0.32% ( $1\sigma$ ). Calibration uncertainties are included in the errors of  $^{238}\text{U}/^{206}\text{Pb}^*$  ratios and dates listed in Table 1. Common-Pb corrections were applied to all analyses using contemporaneous isotopic compositions determined according to the model of Stacey and Kramers (1975).

## Results

Eighty-four analyses were obtained from 78 zircons. Results are listed in Table 1 and shown in a concordia diagram (Fig. 2).



**Figure 1.** Cathodoluminescence image of representative zircons from sample 194777: quartzofeldspathic gneiss, Mount Malcolm. Numbered circles indicate the approximate positions of analysis sites.



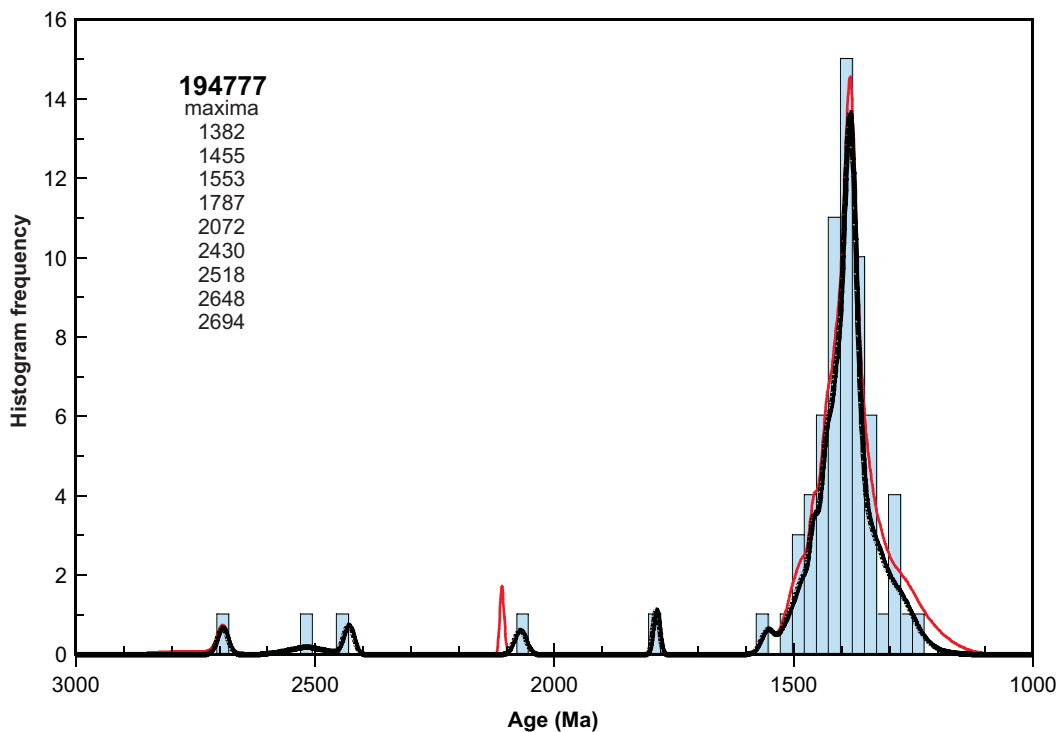
**Figure 2.** U-Pb analytical data for sample 194777: quartzofeldspathic gneiss, Mount Malcolm. Blue square indicates Group Y (youngest detrital zircon); red squares indicate Group S (older detrital zircons); green diamonds indicate Group M (metamorphic zircon rims); crossed squares indicate Group D (discordance >5%).

Table 1. Ion microprobe analytical results for zircons from sample 192505: granitic gneiss, Bishops Road

Group ID	Spot no.	Grain. spot	$^{238}\text{U}$ (ppm)	$^{232}\text{Th}$ (ppm)	$f_{\text{204}}$ (%)	$^{238}\text{U}/^{206}\text{Pb}$ $\pm 1\sigma$	$^{207}\text{Pb}^{*}/^{206}\text{Pb}$ $\pm 1\sigma$	$^{238}\text{U}/^{206}\text{Pb}$ $\pm 1\sigma$	$^{207}\text{Pb}^{*}/^{206}\text{Pb}$ $\pm 1\sigma$	$^{238}\text{U}/^{206}\text{Pb}^{*}$ date (Ma) $\pm 1\sigma$	$^{207}\text{Pb}^{*}/^{206}\text{Pb}^{*}$ date (Ma) $\pm 1\sigma$	Disc. (%)
Y	24	23.1	89	54	0.62	-0.101	4.124	0.068	0.08809	0.00086	4.120	0.068
S	49	45.1	82	50	0.62	0.091	4.129	0.069	0.08775	0.00105	4.133	0.069
S	5	5.1	120	74	0.64	0.165	4.106	0.046	0.08845	0.00080	4.113	0.046
S	57	53.1	158	97	0.63	0.280	4.286	0.059	0.08845	0.00076	4.298	0.059
S	52	48.1	355	206	0.60	-0.059	4.267	0.051	0.08671	0.00061	4.264	0.051
S	63	59.1	118	104	0.91	0.030	4.374	0.064	0.08748	0.00084	4.375	0.064
S	56	52.1	357	199	0.58	0.029	4.313	0.052	0.08760	0.00049	4.314	0.052
S	38	35.2	485	215	0.46	0.048	4.147	0.050	0.08794	0.00041	4.149	0.050
S	19	18.1	381	307	0.83	0.051	4.251	0.052	0.08802	0.00044	4.254	0.052
S	23	22.1	229	177	0.80	-0.014	4.360	0.056	0.08747	0.00056	4.359	0.056
S	3	3.1	113	97	0.89	-0.064	4.210	0.048	0.08712	0.00085	4.208	0.048
S	72	66.1	572	474	0.86	0.062	4.144	0.046	0.08824	0.00037	4.147	0.046
S	17	16.1	248	210	0.87	0.010	4.300	0.054	0.08781	0.00048	4.301	0.054
S	36	34.2	1069	1681	1.62	0.034	4.381	0.051	0.08811	0.00210	4.383	0.051
S	55	51.1	427	293	0.71	0.100	4.296	0.050	0.08869	0.00048	4.300	0.050
S	4	4.1	1019	250	0.25	-0.006	4.263	0.030	0.08786	0.00027	4.263	0.030
S	70	64.1	742	721	1.00	0.004	4.195	0.046	0.08795	0.00033	4.195	0.046
S	21	20.1	220	185	0.87	0.055	4.198	0.054	0.08853	0.00055	4.200	0.054
S	14	13.1	490	330	0.69	-0.014	4.211	0.050	0.08803	0.00032	4.211	0.050
S	69	63.1	566	737	1.34	0.082	4.200	0.046	0.08803	0.00037	4.203	0.047
S	71	65.1	822	802	1.01	-0.013	4.234	0.046	0.08824	0.00032	4.233	0.046
S	29	28.1	233	196	0.87	-0.013	4.233	0.054	0.08837	0.00054	4.233	0.054
S	67	61.1	284	233	0.85	0.013	4.256	0.052	0.08860	0.00056	4.256	0.052
S	32	31.1	837	1653	2.04	0.024	4.218	0.049	0.08876	0.00028	4.219	0.049
S	22	21.1	75	40	0.55	-0.042	4.210	0.067	0.08835	0.00097	4.208	0.067
S	27	26.1	117	89	0.78	0.052	4.110	0.059	0.08837	0.00094	4.112	0.059
S	25	24.1	163	131	0.83	0.093	4.193	0.057	0.08878	0.00065	4.197	0.057
S	51	47.1	85	43	0.52	0.083	4.251	0.069	0.08870	0.00101	4.255	0.069
S	10	9.1	340	337	1.02	0.007	4.202	0.051	0.08817	0.00039	4.202	0.051
S	82	76.1	131	110	0.87	-0.027	4.255	0.060	0.08893	0.00084	4.254	0.060
S	34	33.1	87	103	1.22	-0.068	4.121	0.063	0.08892	0.00091	4.118	0.063
S	9	8.1	95	85	0.93	0.201	4.184	0.059	0.09134	0.00327	4.192	0.059
S	60	56.1	87	70	0.82	0.115	3.918	0.063	0.09020	0.00097	3.922	0.063
S	50	46.1	135	225	1.72	-0.026	4.147	0.059	0.08907	0.00079	4.145	0.059
S	68	62.1	165	152	0.95	-0.062	4.161	0.056	0.08880	0.00071	4.158	0.056
S	31	30	205	124	0.62	0.000	3.970	0.052	0.09007	0.00055	3.970	0.052
S	13	12.1	136	71	0.54	0.035	4.092	0.055	0.09045	0.00063	4.093	0.055
S	76	70.1	189	168	0.92	0.000	4.035	0.053	0.09018	0.00068	4.035	0.053
S	33	32.1	191	107	0.58	0.216	3.919	0.054	0.09256	0.00059	3.927	0.054
S	2	452	288	288	0.66	0.104	4.058	0.032	0.09160	0.00043	4.062	0.032

Table 1. continued

Group	Spot no.	Grain, spot	$^{238}U$ (ppm)	$^{232}Th$ (ppm)	$\frac{^{232}Th}{^{238}U}$	$f^{204}$ (%)	$^{238}U/^{206}Pb$ $\pm 1\sigma$	$^{207}Pb/^{206}Pb$ $\pm 1\sigma$	$^{238}U/^{206}Pb^*$ date (Ma) $\pm 1\sigma$	$^{207}Pb/^{206}Pb^*$ date (Ma) $\pm 1\sigma$	$^{238}U/^{206}Pb^*$ date (Ma) $\pm 1\sigma$	Disc. (%)							
S	64	60.1	144	114	0.82	-0.075	4.199	0.059	0.09052	0.00079	4.196	0.059	0.09116	0.00087	1378	18	1450	18	5.0
S	78	72.1	78	37	0.49	0.125	3.981	0.066	0.09257	0.00104	3.986	0.066	0.09150	0.00121	1443	22	1457	25	1.0
S	16	15.1	503	323	0.66	0.018	3.940	0.222	0.09175	0.00032	3.940	0.222	0.09160	0.00033	1458	77	1459	7	0.1
S	81	75.1	154	99	0.66	0.082	3.897	0.053	0.09303	0.00075	3.900	0.053	0.09232	0.00083	1472	18	1474	17	0.2
S	65	42.2	91	87	0.99	0.098	3.704	0.058	0.09343	0.00094	3.707	0.059	0.09259	0.00106	1540	22	1480	22	-4.1
S	1	1.1	135	123	0.94	-0.144	3.923	0.042	0.09137	0.00077	3.917	0.042	0.09261	0.00092	1466	14	1480	19	1.0
S	53	49.1	84	91	1.12	0.000	3.948	0.065	0.09308	0.00101	3.948	0.065	0.09308	0.00101	1455	22	1490	20	2.3
S	80	74.1	121	53	0.45	-0.024	3.809	0.055	0.09420	0.00080	3.808	0.055	0.09441	0.00083	1503	20	1516	17	0.9
S	66	43.2	206	220	1.10	0.081	3.644	0.047	0.09709	0.00062	3.647	0.047	0.09639	0.00068	1562	18	1555	13	-0.4
S	54	50.1	561	317	0.58	0.014	3.274	0.037	0.10939	0.00040	3.274	0.037	0.10927	0.00040	1718	17	1787	7	3.9
S	6	6.1	105	80	0.78	-0.034	2.668	0.031	0.12777	0.00087	2.667	0.031	0.12807	0.00090	2053	20	2072	12	0.9
S	62	58.1	140	119	0.88	-0.011	2.242	0.033	0.15750	0.00097	2.242	0.033	0.15760	0.00097	2378	29	2430	10	2.2
S	61	57.1	392	372	0.98	-0.004	2.220	0.026	0.16600	0.00414	2.220	0.026	0.16604	0.00414	2397	24	2518	42	4.8
S	58	54.1	73	30	0.42	0.091	1.960	0.033	0.18529	0.00120	1.962	0.033	0.18448	0.00125	2655	37	2694	11	1.4
M	41	38.1	33	93	2.88	0.223	4.525	0.083	0.08388	0.00127	4.535	0.084	0.08199	0.00168	1284	22	1245	40	-3.1
M	47	43.1	39	79	2.12	0.000	4.529	0.082	0.08313	0.00127	4.529	0.082	0.08313	0.00127	1286	21	1272	30	-1.1
M	30	29.1	44	39	0.91	0.065	4.381	0.099	0.08384	0.00116	4.383	0.099	0.08329	0.00129	1325	28	1276	30	-3.8
M	37	35.1	46	74	1.65	0.000	4.515	0.082	0.08374	0.00126	4.515	0.082	0.08374	0.00126	1290	21	1287	29	-0.2
M	35	34.1	52	36	0.72	0.124	4.572	0.080	0.08503	0.00119	4.577	0.081	0.08398	0.00140	1274	21	1292	32	1.4
M	45	41.1	41	63	1.60	0.069	4.597	0.081	0.08488	0.00126	4.600	0.081	0.08429	0.00138	1268	21	1299	32	2.4
M	8	7.1	42	72	1.77	0.227	4.534	0.080	0.08725	0.00127	4.545	0.081	0.08532	0.00169	1282	21	1323	38	3.1
M	28	27.1	150	30	0.21	0.064	4.487	0.061	0.08600	0.00068	4.490	0.061	0.08545	0.00075	1296	16	1326	17	2.2
M	84	78.1	127	79	0.64	0.000	4.167	0.060	0.08551	0.00101	4.167	0.060	0.08551	0.00101	1387	18	1327	23	-4.5
M	79	73.1	59	135	2.38	-0.132	4.520	0.083	0.08507	0.00125	4.514	0.083	0.08619	0.00148	1290	22	1342	33	3.9
M	42	2.2	49	23	0.49	-0.176	4.531	0.076	0.08486	0.00114	4.523	0.076	0.08636	0.00143	1288	20	1346	32	4.4
M	46	42.1	50	62	1.29	0.107	4.515	0.076	0.08730	0.00112	4.520	0.076	0.08638	0.00130	1288	20	1347	29	4.3
M	40	37.1	34	89	2.68	2.807	4.401	0.275	0.11035	0.00156	4.528	0.284	0.08643	0.00487	1286	78	1348	109	4.6
D	44	40.1	29	129	4.51	0.216	4.560	0.091	0.08205	0.00151	4.570	0.092	0.08023	0.00199	1276	24	1203	49	-6.1
D	20	19.1	51	26	0.52	0.463	4.569	0.080	0.08429	0.00118	4.590	0.081	0.08037	0.00190	1271	21	1206	47	-5.3
D	26	25.1	58	44	0.78	-0.114	4.099	0.073	0.08066	0.00135	4.095	0.073	0.08162	0.00151	1409	23	1237	36	-13.9
D	39	36.1	42	115	2.81	0.187	4.370	0.076	0.08409	0.00117	4.378	0.077	0.08251	0.00148	1326	21	1258	35	-5.4
D	48	44.1	45	42	0.98	-0.064	4.620	0.080	0.08533	0.00120	4.617	0.080	0.08588	0.00131	1264	20	1335	30	5.4
D	18	17.1	374	511	1.41	0.027	4.549	0.055	0.08671	0.00044	4.550	0.055	0.08648	0.00046	1281	14	1349	10	5.0
D	43	39.1	25	108	4.49	0.000	4.608	0.095	0.08649	0.00155	4.608	0.095	0.08649	0.00155	1266	24	1349	35	6.1
D	7	6.2	28	134	4.96	-0.095	4.641	0.091	0.08620	0.00143	4.637	0.091	0.08701	0.00165	1259	23	1361	36	7.5
D	12	11.1	31	126	4.22	-0.484	4.448	0.086	0.08445	0.00142	4.427	0.086	0.08858	0.00232	1313	23	1395	50	5.9
D	73	67.1	102	98	0.99	0.182	3.839	0.058	0.09037	0.00087	3.846	0.058	0.08882	0.00108	1490	21	1400	23	-6.4
D	77	71.1	59	63	1.10	0.112	3.814	0.070	0.09097	0.00142	3.818	0.070	0.09001	0.00158	1500	25	1426	33	-5.2
D	59	55.1	98	97	1.02	0.040	4.280	0.067	0.09122	0.00128	4.281	0.067	0.09088	0.00132	1353	19	1444	28	6.3
D	15	14.1	76	42	0.57	0.000	4.162	0.184	0.09348	0.00083	4.162	0.184	0.09348	0.00083	1388	57	1498	17	7.3
D	75	69.1	904	25	0.03	0.009	2.823	0.031	0.13097	0.00032	2.823	0.031	0.13089	0.00033	1955	19	2110	4	7.4
D	74	68.1	128	70	0.56	-0.008	1.611	0.029	0.19103	0.00914	1.610	0.029	0.19111	0.00914	3114	45	2752	79	-13.2



**Figure 3.** Probability density diagram and histogram for sample 194777: quartzofeldspathic gneiss, Mount Malcolm. Thick curve, maxima values, and frequency histogram (bin width 25 Ma) include only data <5% discordant (69 analyses of 64 zircons). Thin curve includes all data (84 analyses of 78 zircons).

## Interpretation

The analyses are concordant to moderately discordant (Fig. 2). Fifteen analyses are >5% discordant (Group D). The dates obtained from these analyses (Group D; Table 1) are unreliable, and are considered not to be geologically significant. The remaining 69 analyses can be divided into three groups, based on their  $^{207}\text{Pb}^*/^{206}\text{Pb}^*$  ratios.

Group Y comprises one analysis of a zircon core (Table 1), which yields a  $^{207}\text{Pb}^*/^{206}\text{Pb}^*$  date of  $1359 \pm 22$  Ma ( $1\sigma$ ).

Group S comprises 55 analyses of zircon cores (Table 1), which yield  $^{207}\text{Pb}^*/^{206}\text{Pb}^*$  dates of 2694–1360 Ma.

Group M comprises 13 analyses of zircon rims (Table 1), which yield a concordia age of  $1304 \pm 13$  Ma (MSWD = 1.9).

It is possible that all of the analyses in Groups Y and S are of unmodified detrital zircons, in which case the date of  $1359 \pm 22$  Ma ( $1\sigma$ ) for the single analysis in Group Y represents a maximum depositional age for the sedimentary precursor. A more conservative estimate of the maximum age of deposition is provided by the weighted mean  $^{207}\text{Pb}^*/^{206}\text{Pb}^*$  date of  $1383 \pm 4$  Ma (MSWD = 0.83) for the 28 youngest analyses in Groups Y and S.

Fifty-five analyses in Group S indicate dates that define significant age components at 1553, 1457, and 1381 Ma, and several minor components between 2694 and 1360 Ma.

These are interpreted as the ages of zircon-crystallizing rocks in the detrital source region(s), or the ages of detrital components within sediments which have been reworked into this rock.

The date of  $1304 \pm 13$  Ma for the 13 analyses in Group M is interpreted as the age of high-grade metamorphism. If the youngest detrital zircon in Group Y was not affected by metamorphism, then deposition of the sedimentary precursor of this rock occurred between c. 1359 and 1295 Ma.

## References

- Clark, DJ, Kinny, PD, Post, NJ and Hensen, BJ 2001, Relationships between magmatism, metamorphism and deformation in the Fraser Complex, Western Australia: constraints from new SHRIMP U–Pb zircon geochronology: Australian Journal of Earth Sciences, v. 46, no. 6, p. 923–932.
- De Waele, B and Pisarevsky, SA 2008, Geochronology, paleomagnetism and magnetic fabric of metamorphic rocks in the northeast Fraser Belt, Western Australia: Australian Journal of Earth Sciences, v. 55, p. 605–621.
- Kirkland, CL, Wingate, MTD and Spaggiari, CV 2011a, 194714: psammitic gneiss, Gnma Hill; Geochronology Record 999: Geological Survey of Western Australia, 6p.
- Kirkland, CL, Wingate, MTD and Spaggiari, CV 2011b, 194715: leucosome in psammitic gneiss, Gnma Hill; Geochronology Record 1000: Geological Survey of Western Australia, 4p.

Spaggiari, CV, Kirkland, CL, Pawley, MJ, Smithies, RH, Wingate, MTD, Doyle, MG, Blenkinsop, TG, Clark, C, Oorschot, CW, Fox, LJ and Savage, J 2011, The geology of the east Albany–Fraser Orogen — a field guide: Geological Survey of Western Australia, Record 2011/23, 98p.

Stacey, JS and Kramers, JD 1975, Approximation of terrestrial lead isotope evolution by a two-stage model: Earth and Planetary Science Letters, v. 26, p. 207–221.

Wingate, MTD and Bodorkos, S 2007, 177910: metamorphosed quartz sandstone, Peters Dam; Geochronology Record 660: Geological Survey of Western Australia, 6p

## Recommended reference for this publication

Kirkland, CL, Wingate, MTD and Spaggiari, CV 2014, 194777: quartzofeldspathic gneiss, Mount Malcolm; Geochronology Record 1160: Geological Survey of Western Australia, 6p.

Data obtained: 1 July 2011

Data released: 31 January 2014